© 1998 Nature America Inc. • http://neurosci.nature.com

Coding of visual information by precisely correlated spikes in the lateral geniculate nucleus

Yang Dan[1,2,3], Jose-Manuel Alonso[2], W. Martin Usrey[1,2] and R. Clay Reid[1,2]

[1] *Department of Neurobiology, Harvard Medical School, Boston, Massachusetts 02115, USA*

[2] *Laboratory of Neurobiology, The Rockefeller University,New York, New York 10021, USA*

[3] *Present address: Department of Molecular and Cell Biology, University of California, Berkeley, California, 94720, USA*

Correspondence should be addressed to R.C.R. (clay_reid@hms.harvard.edu)

Correlated firing among neurons is widespread in the nervous system. Precisely correlated spiking, occurring on a millisecond time scale, has recently been observed among neurons in the lateral geniculate nucleus with overlapping receptive fields. We have used an information-theoretic analysis to examine the role of these correlations in visual coding. Considerably more information can be extracted from two cells if temporal correlations between them are considered. The percentage increase in information depends on the degree of correlation; the average increase is approximately 20% for strongly correlated pairs. Thus, precise temporal correlation could be used as an additional information channel from thalamus to visual cortex.

© 1998 Nature America Inc. • http://neurosci.nature.com

It has been widely accepted that spiking neurons code information in their firing rates[1]. A related assumption is that each neuron serves as an independent channel transmitting information from one stage to another. In principle, however, much more information can be coded in the activity of a neuronal ensemble if temporal correlations between neurons are also used to code additional information not in the isolated spike trains[2]. It remains an important question whether the nervous system uses such distributed codes, and if so, how such 'multiplexed' information is encoded and decoded.

Simultaneous recordings from multiple neurons have shown robust interneuronal correlations within many areas of the brain[2–20]. The functional significance of these temporal correlations, however, remains speculative. The occurrence of correlations depends on features of the sensory inputs[15–17] or the behavioral states of the animal[18,19]. Similarly, different modes of firing of single neurons can be induced by modulatory inputs[21], and it has been suggested that these modes can have distinct roles in information transmission[22]. Such studies may lend insights into the potential roles of temporal correlations in the coding and processing of information.

Neurons in the cat lateral geniculate nucleus (LGN) with overlapping receptive fields show precisely correlated firing[8]. These correlations are faster and often stronger than those previously described in retina, LGN or visual cortex[3–16]: many spikes from pairs of geniculate cells occur nearly simultaneously, with a precision on the order of one millisecond. The existence and strength of the correlation depend on the degree of overlap between the two receptive fields. When the two receptive fields are well overlapped and similar (both X or both Y; both 'on' or both 'off'), they are almost always highly correlated; such pairs typically fire at least 20% of their spikes synchronously. When the cells are of different types (one X, the other Y) or when their centers are only partially overlapped, tightly correlated firing is found among about 10% of pairs and the correlations are much weaker (~2%). As the LGN is the main source of afferent input to the primary visual cortex, these precise temporal correlations could form an important feature of the visual signals received by the cortex. Here we have used a reverse reconstruction technique[23] and information-theoretic analysis[24] to investigate the role of such correlated spiking in visual coding within the LGN. We found that much more information could be extracted from a pair of neurons if the synchronous spikes between them are considered separately. The percentage of increase in information is approximately proportional to the degree of correlation. We therefore conclude that these precise temporal correlations could be used as additional information channels from the LGN to the visual cortex.

Results

A seven-electrode array was used to record the responses from nearby cells (electrode spacing 100–400 μm) in the LGN of the anesthetized cat. For each pair of cells, we calculated the cross-correlogram of their spike trains during white-noise visual stimulation. Between cells with overlapping receptive fields (**Fig. 1a**), we often observed a narrow peak in their cross-correlogram (**Fig. 1b**). These correlations were not due to the time-locking of the two neurons to the visual stimuli, because the peaks were absent in the shuffled correlograms (**Fig. 1b**, solid red line). Among 43 cell pairs with fast (~1 ms) correlations (those with distinct peaks in their cross-correlograms), the strength of correlation (the percentage of spikes that were correlated; see legend to **Fig. 1**) varied continuously between 0.5% and 55%, depending mostly on the degree of overlap between the two receptive fields.

Coding of visual information by correlated spikes

To investigate the potential role of these correlations in information coding, we sorted the spikes of each cell pair into three categories: spikes that were synchronous between A and B (A&B),

© 1998 Nature America Inc. • http://neurosci.nature.com

spikes of A that were nonsynchronous with B (A*), and spikes of B that were nonsynchronous with A (B*). The original spike trains of the two neurons in Fig. 1 (A and B) had a high percentage of near-synchronous spikes between them (**Fig. 2a**). After sorting these two spike trains into the three derived spike trains A&B, A* and B* (**Fig. 2b**), we sought to determine whether we could extract more information from these three derived spike trains than from the two original spike trains, that is, whether more can be learned about the stimulus if the synchronous spikes are considered separately.

First, we calculated the first-order spatiotemporal receptive field (Wiener kernel)[25,26] for each spike train (**Fig. 3**, left column). This form of receptive-field analysis has been used on correlated cells in the retina[7] and the visual cortex[14]. The differences between the original receptive fields (A and B) and the derived receptive fields (A&B, A* and B*) are slight, but important. The center of the bicellular receptive field[14] (A&B) is confined to the area where the original receptive fields were strongest (up and to the right), whereas the receptive fields of the isolated spikes (A* and B*) are relatively stronger at positions lower and to the left.

Second, we did an information-theoretic analysis on the original and derived spike trains to determine whether the extremely strong correlation between thalamic neurons might carry information about the stimulus. For each pixel, we reconstructed the visual input (white noise) with the reverse reconstruction technique[23] and calculated mutual information between the input and the reconstruction at each pixel using information theory[24]. This calculation yields a lower bound of the mutual information between stimulus and responses that depends on the method of reconstruction[23]. We created 'information maps' that represent the time-averaged mutual information between the spike trains and the stimulus at each pixel (**Fig. 3**, middle column), based on the reconstruction from two spike trains (A and B) and from three spike trains (A&B, A* and B*). We plotted the difference between these two maps at a different scale (×6; **Fig. 3**, right column). An increase in information was found in a region approximately corresponding to the centers of the receptive fields of A and B. For these pixels, the reconstruction of the stimulus from the three derived spike trains was better than that from the two original spike trains. Note that the greatest increase in information was at the pixels, down and to the left, where the receptive fields of the isolated spikes (A* and B*) were relatively stronger than those of the original spike trains (A and B).

To evaluate the overall increase in information for each cell pair, we calculated the sum of information over all pixels for both the two-spike-train reconstruction and the three-spike-train reconstruction. Even though this sum does not represent the total mutual information between the reconstructed and the actual visual inputs, the ratio between these sums provides a useful heuristic measure of the overall increase in information. This ratio between the information sums is equivalent to the average information ratio for each pixel, weighted by the original (two spike train) information at each pixel. The percentage increase in information showed a definite dependence on the strength of correlation (**Fig. 4a**). For 43 pairs of cells, the correlation coefficient between the percentage of increase in information and the strength of correlation was 0.70. The slope of the linear regression was 0.41.

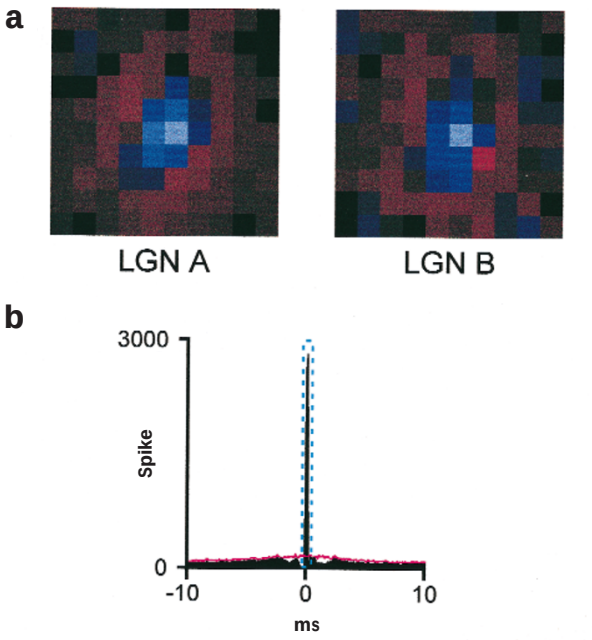

Fig. 1. Correlated spiking between geniculate neurons with overlapping receptive fields. **(a)** Receptive fields of two simultaneously recorded off-center cells, A and B, mapped with white-noise input and reverse correlation method[25,26]. Red, 'on' responses; blue, 'off' responses. The brightest colors correspond to the strongest responses. 0.4 degrees/pixel. Delay shown, 23 milliseconds. The centers of the two receptive fields were well overlapped. **(b)** Cross-correlograms between the two cells during white-noise stimulation (black histogram). The dotted blue lines show the boundaries of the peak, –0.2 to 0.3 milliseconds, which were used to derive the three spike trains in Fig. 2b. The strength of correlation (15.8%) was defined as the number of spikes in the peak of the correlogram, minus the baseline, divided by the average of the total number of spikes produced by each neuron[8]. The solid red line is the shuffled correlogram[36]: The same white-noise input was repeated twice, resulting in spike trains *A1, B1* and *A2, B2* (*A* and *B* represent the two LGN neurons, *1* and *2* represent the two repeats of the same stimuli), then *A1* was correlated with *B2*, and *A2*, with *B1*. The total numbers of spikes in the two repeats were 18,697 and 17,556 for cells A and B, respectively. Data were collected over a period of 16 minutes.

Control analyses

To further establish the causal relationship between correlated spiking and efficient visual coding, we did four control analyses. First, we analyzed 20 pairs of cells that had partially overlapping receptive fields but were uncorrelated. Although there was no distinct peak in their cross-correlograms, the central bins were non-zero, that is, there were 'randomly' synchronous spikes. We derived the three spike trains by considering these randomly synchronous spikes as A&B. As would be expected from the modest increase in information for weakly correlated pairs (**Fig. 4a**), random correlations did not result in a significant increase in information compared to the two original spike trains (1.97 ± 3.67%, standard deviation, $p > 0.2$, Wilcoxon). This indicates that the increase in information depends on the nonrandom, precise correlations between geniculate cells.

For finite data samples, merely increasing the number of categories, or degrees of freedom, can produce a better reconstruction and additional information. Because dividing two spike trains into three added a degree of freedom to the reconstruction, the increase in information we observed might therefore have been an artifact of creating this degree of freedom. To exclude this possibility, we carried out a second control analysis.

© 1998 Nature America Inc. • http://neurosci.nature.com

© 1998 Nature America Inc. • http://neurosci.nature.com

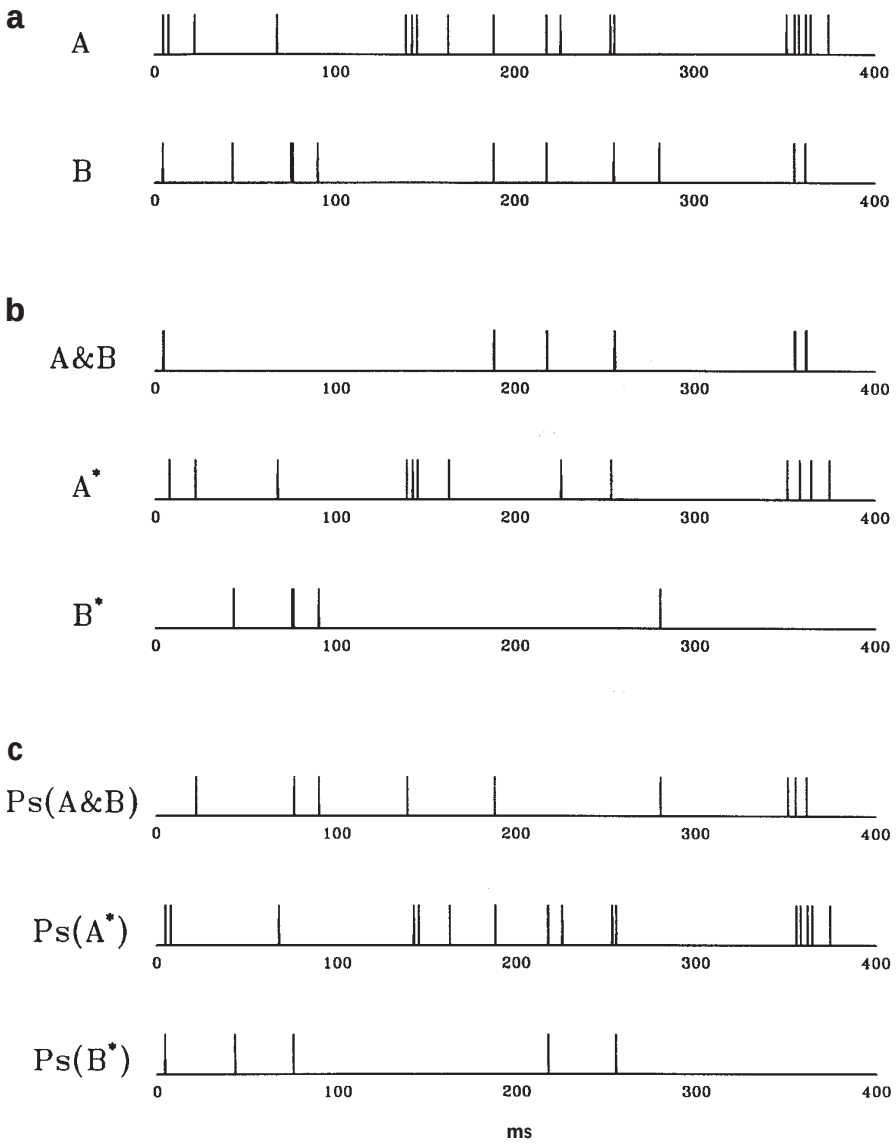

Fig. 2. Spike-sorting procedure. **(a)** A and B are segments of the original spike trains of the two cells in Fig. 1, during white-noise stimuli. For these highly correlated pairs, there were many near-synchronous spikes. **(b)** The three derived spike trains were as follows: synchronous spikes between A and B (A&B), and spikes in either cell that were nonsynchronous with the other (A* and B*). The sorting of spike trains was based on the correlogram between A and B (**Fig. 1b**). The left and right boundaries of the peak were determined visually, and all the spikes that fell within this window were classified as A&B. The dotted red lines in Fig. 1b show the boundaries of the window for those two cells, –0.2 to 0.3 milliseconds. **(c)** The three randomly derived spike trains for the control analysis. The number of synchronous spikes in A&B shown in (b) was counted, then the same number of spikes was taken out randomly from A and B to form pseudo (Ps) (A&B). The rest of spikes in A and B formed Ps(A*) and Ps(B*), respectively.

For each pair of cells, we counted the number of synchronous spikes that were taken out to form A and B. We then took out the same number of spikes, but randomly, from A and B to form a 'pseudo A&B' (**Fig. 2c**). This manipulation did not result in a systematic increase in information (**Fig. 4b**). We did a paired nonparametric test between the data shown in Fig. 4a and those in 4b. These two populations were significantly different ($p < 5 \times 10^{-7}$, Wilcoxon). Thus, the observed increase in information was not an artifact of adding a degree of freedom to the reconstruction. Adding a degree of freedom actually tended to decrease the information in Fig. 4b. A decrease in information might be expected, given that information is lost when spikes from two neurons are randomly lumped together. The analysis ensures, however, that this effect is not overpowered by an increase in information from an added degree of freedom.

So far, we have shown that more information can be extracted from a pair of correlated neurons if we consider the synchronous spikes separately. This does not prove, however, that a correlated pair of cells carries more information than a similar, uncorrelated pair. Although correlations can carry information, they might also cause redundancy[24]. It is possible therefore that the gain of information we observed was offset by a loss of information because of correlation-induced redundancy. A third control analysis was done to assess this potential redundancy. For six pairs of cells, we repeated the same white-noise input twice, resulting in the responses A1, B1 and A2, B2. We then compared the information from the direct pairings A1, B1 and A2, B2 to that from crossed (shuffled) pairings A1, B2 and A2, B1. In this analysis, only the original spike trains were used; we did not sort spikes into three categories to extract the additional information carried by the correlations. Because the precise correlation was not observed in shuffled correlograms (**Fig. 1b**, solid red line), the potential redundancy was eliminated in the crossed pairings. Therefore, A1, B2 and A2, B1 might have easily provided more information than A1, B1 and A2, B2. The difference in information between the former and the latter groups was defined as the correlation-induced redundancy. For these six pairs of cells, whose strength of correlation ranged from 5.3% to 34.9%, the correlation-induced redundancy was insignificant (–1.37 ± 2.21%, standard deviation). Thus, the only effect of the precise correlation was to enhance the efficiency of coding, as shown above.

Finally, to prove that the increase in information was caused by the precise correlation in the LGN and not by the slower correlations found in the retina[2–7], we studied the relationship

© 1998 Nature America Inc. • http://neurosci.nature.com

© 1998 Nature America Inc. • http://neurosci.nature.com

between the increase in information and the window size. If the origin of the increase in information is the slower correlation in the retina, we should expect to extract more information when we include more correlated spikes in A&B with a bigger window size. When we defined spike train A&B with window sizes 1, 5, 10, 20 and 40 ms, the average increases in information for the 43 pairs of cells were 11.1 ± 9.0%, 6.5 ± 9.1%, 6.3 ± 9.6%, 5.4 ± 9.7%, and 4.0 ± 13.6%, respectively. Thus, increasing the window size did not result in more increase in information. These results indicate that the increase in information is caused specifically by the precise correlation in the LGN and not by the slower correlations in the retina.

Discussion

We have shown that for a pair of correlated cells, information can be increased by considering the synchronous spikes explicitly. This gain was relative to decoding based purely on firing rate, in which the information carried by a neuron is reconstructed based on its first-order receptive field. In a linear rate code, the optimal estimate of the input preceding each spike is given by the reverse filter for each neuron[23]. Here we have instead sorted the spikes of each neuron into different categories based on their temporal relationship with spikes of a neighboring neuron. The first-order receptive field and reverse filter for each category of spikes were calculated separately. Therefore we assigned different 'meanings' to the spikes in different categories. The increase in information observed in our analysis indicates that this 'correlation code' has a higher information capacity than the pure rate code. However, our simple analysis (essentially a linear rate code for the three derived spike trains) is likely to provide a lower estimate of the potential increase in information. More elaborate nonlinear analysis may demonstrate even more information in the neuronal ensemble.

Previous studies that examined the receptive fields of correlated firing ('bicellular receptive fields') both in the visual cortex[14] and in the retina[7] found that the receptive fields of the correlated spikes were different from the receptive fields of the individual neurons. Here, in addition to a receptive-field analysis, we have also done an information-theoretic analysis to examine the information contained in correlated firing. The pairs of cells we studied in the LGN differ from those in previous studies in that the correlations are stronger and faster[8] (and therefore are not 'inherited' from retinal correlations[2–7]), and the receptive fields (including the bicellular receptive field) are more similar. Despite the potential redundancy that could have resulted from both the similarity of all three receptive fields and the correlations themselves, we found that the uniquely strong correlated activity in the LGN carries information. Previously, we have found that the precisely correlated spiking in the LGN is caused by divergent inputs from retinal ganglion cells[8,27], as has been predicted from past studies[28–30]. This knowledge may provide some insight into the results presented here. The synchronous spike train (A&B) is presumably a subset of the spike train of the common presynaptic retinal ganglion cell(s). Geniculate neurons can have different response properties from their retinal inputs[31,32]. Therefore, the partial presynaptic spike train (represented by A&B), which has a different spatiotemporal receptive field, may provide an additional, dis-

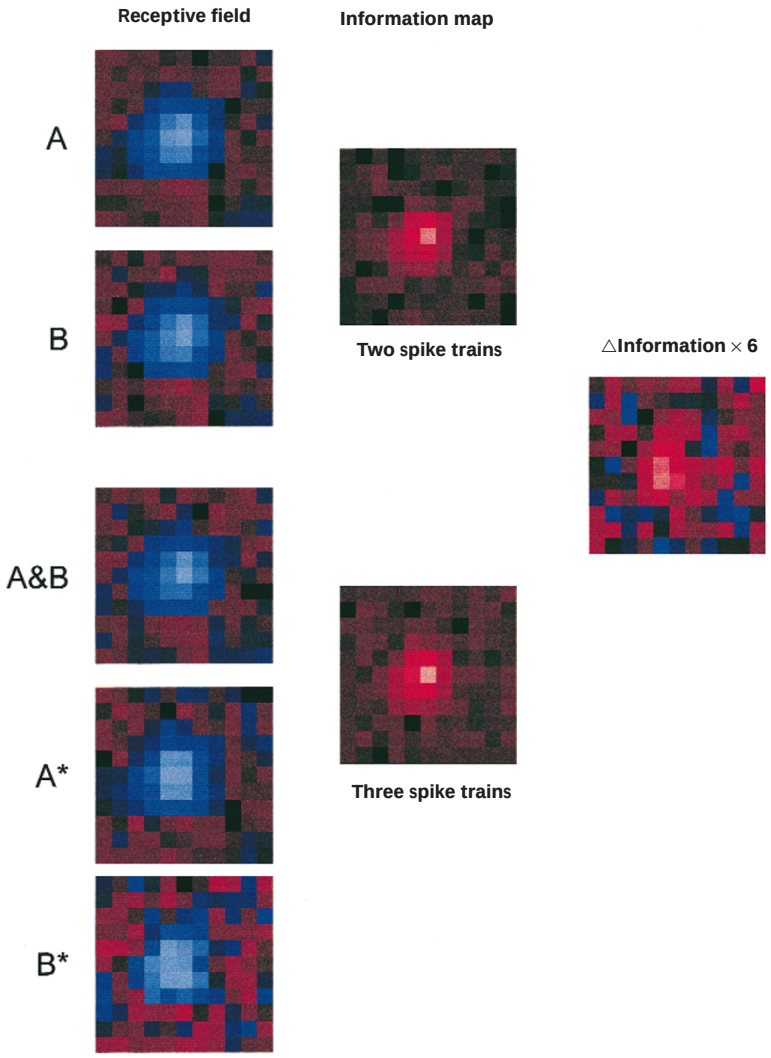

Fig. 3. Gain of information by considering the correlation between a pair of cells. Left column, first-order receptive fields of the original spike trains, A and B, and the derived spike trains, A&B, A*, and B*. Red, 'on' responses; blue, 'off' responses. 0.4 degrees/pixel. Delay shown, 27 milliseconds. The receptive fields of the two original spike trains were well overlapped and the two cells were strongly correlated (strength, 43.1%). Middle column, the information map based on the two original spike trains (A and B), and that based on the three derived spike trains (A&B, A*, and B*). The mutual information between the actual input and the reconstruction is indicated by the brightness at each pixel. Maximum, 2.3 bit/s. Right column, the difference between the information map of the three spike trains and that of the two spike trains. Red, positive; blue, negative. Values in the difference map (maximum, 0.38 bits/s) were multiplied by six and plotted on the same scale. Considerable increase in information was only found in the pixels within the receptive fields of these cells. The small differences (both positive and negative) seen in pixels outside of this region were noise.

© 1998 Nature America Inc. • http://neurosci.nature.com

© 1998 Nature America Inc. • http://neurosci.nature.com

tinct estimate of the visual input.

The intrageniculate correlations we studied are stronger and more precise than other correlations observed within a single level in the cat visual system[33] whether between cortical cells[10–15,20], between geniculate cells with non-overlapping receptive fields[9,16], or between retinal ganglion cells[3–6]. (In the cat retina, the fastest correlations between pairs of cells have two peaks, ~1 ms on either side of zero[6], although such correlations are faster in the salamander[34].) The faster thalamic correlations studied here may be particularly well suited for presenting to the cortex the information relayed from the retina. Because the spike trains of retinal ganglion cells carry information at very high rates, an important function of the LGN may be to distribute, or multiplex, this information into both single-cell-based and correlation-based channels to facilitate further processing in the cortex.

Precisely correlated spiking is a robust phenomenon in the LGN; more than half of the well overlapped pairs, as well as a smaller percentage of partially overlapped pairs, showed significant correlations[8]. Because each geniculate neuron will be correlated with a small ensemble of other neurons, there are more potential information channels based on pairwise correlations than those based on single cells. Given any potential information channel, the ultimate test of the importance of a neural code is whether it is available for further processing. The advantage of a correlation-based information channel is its easy accessibility for the next stage of processing. Simultaneous recordings in the LGN and the cortex have in fact shown that synchronous spikes from the LGN are more efficient in driving their cortical targets[8]. Such coincidence-detection mechanisms in the postsynaptic cortical cell may provide a means for 'reading out' the temporal code we have found in the LGN.

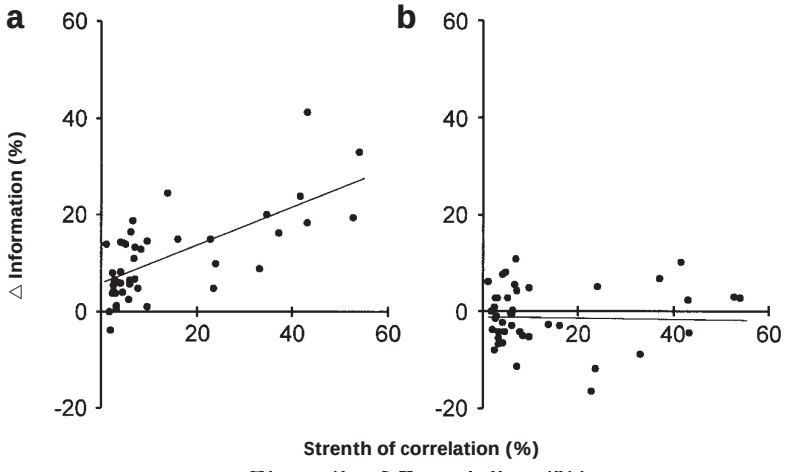

Fig. 4 Dependence of increase in information on strength of correlation. **(a)** Increase in information was plotted against strength of correlation for 43 pairs of cells. Each point represents data from one pair. The ratio between information (summed over all pixels) for the three-spike-train reconstruction and that for the two-spike-train reconstruction was calculated. Increase in information was defined as this ratio minus one. The strength of correlation is defined in the legend of Fig. 1. The solid line is the linear regression of all points (slope, 0.41; intercept, 5.5%; $r = 0.70$). **(b)** Change in information by taking out the same number of spikes, but randomly (pseudo A&B), from the cell pairs shown in (a). The solid line is the linear regression (slope, –0.006; intercept, –1.1%; $r = –0.01$).

Methods

PHYSIOLOGICAL PREPARATION. Adult cats, ranging in weight from 2 to 3 kg, were initially anesthetized with ketamine HCl (20 mg/kg, intramuscular), followed by sodium pentothal (20 mg/kg, intravenous; supplemented as needed). A local anesthetic (lidocaine) was injected before all incisions. Anesthesia was maintained for the duration of the experiment with sodium pentothal at a dosage of 6 mg/hr. A tracheotomy was done to allow artificial ventilation. Then the cat was transferred to a Horsley-Clarke stereotaxic frame. To minimize respiratory movements, the cat was suspended by clamping the spinous process of one of the lumbar vertebrae. The animal was paralyzed with norcuron and artificially ventilated. Ventilation was adjusted so that the end-expiratory CO_2 was near 3.5%. Core body temperature was monitored and maintained at 38°C. EKG and EEG were also monitored continuously.

Pupils were dilated with topical application of 1% atropine sulfate, and the nictitating membranes were retracted with 10% phenylephrine. Eyes were refracted, fitted with appropriate contact lenses and focused on a tangent screen. The positions of the areae centrales were plotted with the aid of a fundus camera. Eyes were stabilized mechanically by gluing them to metal posts attached to the stereotaxic apparatus. A craniotomy (about 0.5 cm in diameter) was made over the LGN and the underlying dura removed. The hole was filled with 3% agar in physiological saline to improve stability of the recordings.

ELECTROPHYSIOLOGICAL RECORDING. Neighboring geniculate cells were recorded with multielectrodes (Thomas Recording, Marburg, Germany). The array allows seven fiber electrodes to be positioned independently with a vertical accuracy of 1 µm. We used a glass guide tube to restrict the lateral scatter of the electrodes in the array. The inner diameter at the tip of the guide tube was less than 400 µm. All recordings were made in layer A or A1 of the LGN.

Recorded signals were amplified, filtered and passed to an 80486 PC running Datawave Discovery software (Datawave Systems, Broomfield, Colorado). The system accepts inputs from up to eight single electrodes. Up to eight different waveforms can be discriminated on a single electrode, but two to three is a more realistic limit. The waveforms of the spikes were saved on disk. Spike isolation was based on cluster analysis of waveforms, and presence of a refractory period was based on the shape of autocorrelations. The spike discrimination was first done approximately during the experiment. The sorting was done more rigorously in post-processing. All pairs of neurons were recorded on different electrodes.

VISUAL STIMULATION. The data-acquisition PC contained an AT-Vista graphics card (Truevision, Indianapolis, Indiana), which was used to present visual stimuli at a frame rate of 128 Hz. The stimulus was updated either every frame, every other frame or (occasionally) every four frames. All stimuli were programmed using subroutines from a 'runtime' library, YARL (written by Karl Gegenfurtner). The system is well suited for the efficient real-time production of spatiotemporal white-noise stimuli using an m-sequence temporal signal[25,26]. Spatially, the white-noise stimuli were made up of 16×16 grids of square regions (pixels). The pixel sizes were adjusted to map receptive fields with a reasonable level of detail (0.2–0.4 degrees at 5–10 degrees eccentricity). For every frame of the stimulus, the pixels were either black (–1) or white (+1) according to the m-sequence. The full m-sequence was of length $2^{15} - 1 = 32{,}767$, for a total of four minutes when updated every frame, or eight minutes when updated every other frame. Usually, several repeats of the four- or eight-minute stimulus were done. The receptive field maps of the neurons were calculated using the reverse correlation method[25,26]. For each delay between stimulus onset and nerve impulse firing, the average spatial stimulus that preceded each impulse was calculated. This calculation was done with the fast m-transform[25].

© 1998 Nature America Inc. • http://neurosci.nature.com

© 1998 Nature America Inc. • http://neurosci.nature.com

DATA ANALYSIS: REVERSE RECONSTRUCTION. For each pixel, the input was reconstructed based on either the two original spike trains (A and B) or the three derived spike trains (A&B, A* and B*). For two spike trains, the reverse filters $H_{1,j}$ and $H_{2,j}$ were obtained by solving the following linear equations in the frequency domain:

$$\begin{pmatrix} |R_1|^2 & \bar{R}_1 \cdot R_2 \\ R_1 \cdot \bar{R}_2 & |R_2|^2 \end{pmatrix} \begin{pmatrix} H_{1,j} \\ H_{2,j} \end{pmatrix} = \begin{pmatrix} \bar{K}_{1,j} \\ \bar{K}_{2,j} \end{pmatrix} \quad (1)$$

where j is the index for the pixel; R_1 and R_2 are the responses of the two cells in the frequency domain, calculated by binning the spike trains followed by a Fourier transform; $\bar{R}_1$ and $\bar{R}_2$ are the complex conjugates of R_1 and R_2; $|R_1|^2$ and $|R_2|^2$ are the power spectra; $K_{1,j}$ and $K_{2,j}$ are temporal Fourier transforms of the first-order receptive fields (Wiener kernels[25,26]) of the two cells at the 'jth' pixel; and $\bar{K}_{1,j}$ and $\bar{K}_{2,j}$ are their complex conjugates.

The reverse filters $H_{1,j}$ and $H_{2,j}$ that satisfy these equations are

$$H_{1,j} = \frac{\det\begin{pmatrix} \bar{K}_{1,j} & \bar{R}_1 \cdot R_2 \\ \bar{K}_{2,j} & |R_2|^2 \end{pmatrix}}{\det\begin{pmatrix} |R_1|^2 & \bar{R}_1 \cdot R_2 \\ R_1 \cdot \bar{R}_2 & |R_2|^2 \end{pmatrix}}, \quad H_{2,j} = \frac{\det\begin{pmatrix} |R_1|^2 & \bar{K}_{1,j} \\ R_1 \cdot \bar{R}_2 & \bar{K}_{2,j} \end{pmatrix}}{\det\begin{pmatrix} |R_1|^2 & \bar{R}_1 \cdot R_2 \\ R_1 \cdot \bar{R}_2 & |R_2|^2 \end{pmatrix}} \quad (2)$$

The reconstruction of the stimulus at the 'jth' pixel, S^{r2}_j, is given in the frequency domain by

$$S^{r2}_j = H_{1,j}R_1 + H_{2,j}R_2 \quad (3)$$

The reconstruction in the time domain, $s^{r2}_j(t)$, is the inverse Fourier transform of S^{r2}_j. These reconstructions are optimal in the sense that they minimize the chi-squared difference between the reconstruction and the actual input, given the spike trains and their measured first-order receptive fields.

For three spike trains, the reverse filters $H_{1,j}$, $H_{2,j}$ and $H_{3,j}$ were obtained similarly by solving the following linear equations

$$\begin{pmatrix} |R_1|^2, & \bar{R}_1 \cdot R_2, & \bar{R}_1 \cdot R_3, \\ R_1 \cdot \bar{R}_2, & |R_2|^2, & \bar{R}_2 \cdot R_3, \\ R_1 \cdot \bar{R}_3, & R_2 \cdot \bar{R}_3, & |R_3|^2, \end{pmatrix} \begin{pmatrix} H_{1,j} \\ H_{2,j} \\ H_{3,j} \end{pmatrix} = \begin{pmatrix} \bar{K}_{1,j} \\ \bar{K}_{2,j} \\ \bar{K}_{3,j} \end{pmatrix} \quad (4)$$

The reconstruction of the stimulus in the frequency domain is given by

$$S^{r3}_j = H_{1,j}R_1 + H_{2,j}R_2 + H_{3,j}R_3 \quad (5)$$

The reconstruction in the time domain $s^{r3}_j(t)$ is the inverse Fourier transform of S^{r3}_j.

DATA ANALYSIS: MUTUAL INFORMATION. The mutual information between the actual visual input s_j and the reconstruction s^r_j was calculated by making a joint probability table between them. Because the input at each pixel was binary white noise (an m-sequence[25,26]), it had only two values: 1 or –1. The reconstructed input was a continuous variable that was quantized into 100 bins. The joint probability table therefore had 200 entries. The probability was calculated by counting the number of events for each entry normalized by the total number of events in the input sequence, which in our experiment was 32,767. The mutual information between the reconstructed and the actual stimuli at the jth pixel $I(s^r_j, s_j)$ was calculated based on the equation:

$$I(s^r_j, s_j) = \sum_{s,s'} P(s^r_j, s_j) \log \frac{P(s^r_j, s_j)}{P(s^r_j)\,P(s_j)} \quad (6)$$

where $P(s^r_j, s_j)$ is the joint probability between s^r_j and s_j, and $P(s^r_j)$ and $P(s_j)$ are the probability distributions of s^r_j and s_j, respectively. This mutual information is a statistical average over time.

To correct for the overestimation of information caused by a finite number of events, we used a method developed by Panzeri and Treves[35]. The final estimate of mutual information was given by $I(s^r_j, s_j)$, calculated as above, minus a correction term (ref. 35, Eq. 6). To prove directly that we were not 'over-fitting', for nine pairs of cells for which we recorded two repeats of the white-noise stimuli, we calculated the reverse filters from one repeat and reconstructed the stimuli from the other repeat. (The repeats were interleaved, to avoid effects from 'non-stationarity.') The mutual information was then calculated in the same manner as in the original analysis. The difference in information between the cross-validation and the original analysis was not significant. The average difference in information was 0.23 + 2.8% for the two original spike trains, 0.53 + 2.8% for the three derived spike trains.

To evaluate the overall increase in information caused by spike-train sorting, we calculated the sum of information over all pixels for both the two-spike-train reconstruction and the three-spike-train reconstruction. However, this sum, $\sum_j I(s^r_j, s_j)$ is less than the total mutual information between the complete spatiotemporal white-noise input and the reconstruction, $I(s^r_1, s^r_2, \ldots s^r_j \ldots; s_1, s_2, \ldots s_j \ldots)$. This is because the reconstructions of the inputs at different pixels are correlated, so the reconstruction at any pixel, s^r_j, may carry information not only about s_j, but also about stimuli at neighboring pixels. Thus, summing the information between the actual and the reconstructed signals at each pixel may yield an underestimate of the total information carried by the spike trains. However, as there is no correlation between the actual stimuli at different pixels, s_i and s_j, this sum can never overestimate the total information. In our analyses, evaluation of the total mutual information is impossible because of the finite data set. The sum of mutual information over all pixels, however, provides a useful measure to compare the information present in different reconstructions.

Acknowledgements

We are grateful to T. Wiesel for his support during the early phase of this work. K. Gegenfurtner allowed us to use his library of subroutines, YARL, to write programs for our visual stimuli. Technical assistance was provided by K. McGowan, C. Gallagher and D. Landsberger. The research was supported by NIH EY05253, EY06604, EY10115, the Klingenstein Fund, Fulbright/MEC and the Charles H. Revson Foundation. Y.D. was a Schering-Plough Fellow of the Life Sciences Research Foundation.

RECEIVED 13 JULY; ACCEPTED 19 AUGUST 1998

1. Adrian, E. D. *The Basis of Sensation* (W.W. Norton, New York, 1928).
2. Meister, M. Multineuronal codes in retinal signaling. *Proc. Natl. Acad. Sci. USA* **93**, 609–614 (1996).
3. Rodieck, R. W. Maintained activity of cat retinal ganglion cells. *J. Neurophysiol.* **30**, 1043–1071 (1967).
4. Mastronarde, D. N. Correlated firing of cat retinal ganglion cells. I. Spontaneously active inputs to X- and Y-cells. *J. Neurophysiol.* **49**, 303–324 (1983).
5. Mastronarde, D. N. Correlated firing of cat retinal ganglion cells. II. Responses of X- and Y-cells to single quantal events. *J. Neurophysiol.* **49**, 325–349 (1983).
6. Mastronarde, D. N. Interactions between ganglions cells in cat retina. *J. Neurophysiol.* **49**, 350–365 (1983).
7. Meister, M., Lagnado, L. & Baylor, D. A. Concerted signaling by retinal ganglion cells. *Science* **270**, 1207–1210 (1995).
8. Alonso, J. M., Usrey, W. M. & Reid, R. C. Precisely correlated firing in cells of the lateral geniculate nucleus. *Nature* **383**, 815–819 (1996).
9. Sillito, A. M., Jones, H. E., Gerstein, G. L. & West, D. C. Feature-linked synchronization of thalamic relay cell firing induced by feedback from the visual cortex. *Nature* **369**, 479–482 (1994).
10. Toyama, K., Kimura, M. & Tanaka, K. Cross-correlation analysis of interneuronal connectivity in cat visual cortex. *J. Neurophysiol.* **46**, 191–201 (1981).
11. Ts'o, D. Y., Gilbert, C. D. & Wiesel, T. N. Relationships between horizontal interactions and functional architecture in cat striate cortex as revealed by cross-correlation analysis. *J. Neurosci.* **6**, 1160–1170 (1986).
12. Eckhorn, R. *et al.* Coherent oscillations: a mechanism of feature linking in the visual cortex? Multiple electrode and correlation analyses in the cat. *Biol. Cybern.* **60**, 121–130 (1988).
13. Nelson, J. I., Salin, P. A., Munk, M. H. J., Arzi, M. & Bullier, J. Spatial and temporal coherence in cortico-cortical connections: a cross-correlation study in areas 17 and 18 in the cat. *Vis. Neurosci.* **9**, 21–37 (1992).
14. Ghose, G. M., Ohzawa, I. & Freeman, R. D. Receptive-field maps of correlated discharge between pairs of neurons in the cat's visual cortex. *J. Neurophysiol.* **71**, 330–346 (1994).

© 1998 Nature America Inc. • http://neurosci.nature.com

© 1998 Nature America Inc. • http://neurosci.nature.com

15. Singer, W. & Gray, C. M. Visual feature integration and the temporal correlation hypothesis. *Annu. Rev. Neurosci.* **18**, 555–586 (1995).
16. Neuenschwander, S. & Singer, W. Long-range synchronization of oscillatory light responses in the cat retina and lateral geniculate nucleus. *Nature* **379**, 728–732 (1996).
17. deCharms, R. C. & Merzenich, M. M. Primary cortical representation of sounds by the coordination of action-potential timing. *Nature* **381**, 610–613 (1996).
18. Abeles, M., Bergman, H., Margalit, E. & Vaadia, E. Spatiotemporal firing patterns in the frontal cortex of behaving monkeys. *J. Neurophysiol.* **70**, 1629–1638 (1993).
19. Murthy, V. N. & Fetz, E. E. Coherent 25- to 35-Hz oscillations in the sensorimotor cortex of awake behaving monkeys. *Proc. Natl Acad. Sci. USA*. **89**, 5670–5674 (1992).
20. Swadlow, H. A., Beloozerova, I. N. & Sirota, M. G. Sharp, local synchrony among putative feed-forward inhibitory interneurons of rabbit somatosensory cortex. *J. Neurophysiol.* **79**, 567–582 (1998).
21. Guido, W., Lu, S. M., Vaughan, J. W, Godwin, D. W. & Sherman, S. M. Receiver operating characteristic (ROC) analysis of neurons in the cat's lateral geniculate nucleus during tonic and burst response mode. *Vis. Neurosci.* **12**, 723–741 (1995).
22. Sherman, S. M. Dual response modes in lateral geniculate neurons: mechanisms and functions *Vis. Neurosci.***13**, 205–213 (1997).
23. Bialek, W., Rieke, F., de Ruyter van Steveninck, R. R. & Warland, D. Reading a neural code. *Science* **252**, 1854–1857 (1991).
24. Shannon, C. E. & Weaver, W. *The Mathematical Theory of Communication* (Univ. Illinois, Chicago, 1963).
25. Sutter, E. E. in *Advanced Methods of Physiological Systems Modeling,* Vol. **1**, (ed V. Marmarelis) 303–315 (Univ. Southern California, Los Angeles, 1987).
26. Reid, R. C., Victor, J. D. & Shapley, R. M. The use of m-sequences in the analysis of visual neurons: Linear receptive field properties. *Vis. Neurosci.* **14**, 1015–1027 (1997).
27. Usrey, W. M, Reppas, J. B. & Reid, R. C. Paired-spike interactions and synaptic efficacy of retinal inputs to thalamus. *Nature* (in press).
28. Cleland B. G., Dubin M. W. & Levick W. R. Simultaneous recording of input and output of lateral geniculate neurones. *Nature* **231**, 191–192 (1971).
29. Cleland B. G., Dubin M. W. & Levick W. R. Sustained and transient neurones in the cat's retina and lateral geniculate nucleus. *J. Physiol.* **217**, 473–496 (1971).
30. Cleland B. G. in *Visual Neuroscience* (eds Pettigrew, J. D., Sanderson, K. S. & Levick, W. R) 111–120 (Cambridge Univ. Press, London, 1986).
31. Hubel, D. H. & Wiesel, T. N. Integrative action in the cat's lateral geniculate body. *J. Physiol.* **155**, 385–398 (1961).
32. Kaplan E., Purpura K. & Shapley R. M. Contrast affects the transmission of visual information through the mammalian lateral geniculate nucleus. *J. Physiol.* **391**, 267–288 (1987).
33. Usrey, W. M. & Reid, R. C. Synchronous activity in the visual system. *Annu. Rev. Physiol.* **61** (in press).
34. Brivanlou I. H., Warland, D. K. & Meister M. Mechanisms of concerted firing among retinal ganglion cells. *Neuron* **20**, 527–539 (1998).
35. Panzeri, S. & Treves, A. Analytical estimates of limited sampling biases in different information measures. *Network: Computation in Neural Systems* **7**, 87–107 (1996).
36. Perkel, D. H., Gerstein, G. L. & Moore, G. P. Neuronal spike trains and stochastic point processes. II. Simultaneous spike trains. *Biophys. J.* **7**, 419–440 (1967).

© 1998 Nature America Inc. • http://neurosci.nature.com